Peng Cheng
e-mail: pc2052@columbia.edu

Yajun Fan

Jie Zhang

Y. Lawrence Yao

Department of Mechanical Engineering,
Columbia University,
New York, NY 10027

David P. Mika

Wenwu Zhang

Michael Graham

Jud Marte

Marshall Jones

Global Research Center,
General Electric Company,
Niskayuna, NY

Laser Forming of Varying Thickness Plate—Part II: Process Synthesis

Laser forming (LF) is a non-traditional forming process that does not require hard tooling or external forces and, hence, may dramatically increase process flexibility and reduce the cost of forming. While extensive progress has been made in analyzing and predicting the deformation given a set of process parameters, few attempts have been made to determine the laser scanning paths and laser heat conditions given a desired shape. This paper presents a strain-based strategy for laser forming process design for thin plates with varying thickness, which is utilized in determining the scanning paths and the proper heating conditions. For varying thickness plates, both the in-plane membrane strain and the bending strain need to be accounted for in process design. Compared with uniform thickness plate, the required bending strain varies with not only the shape curvature but also with the plate thickness. The scanning paths are determined by considering the different weight of bending strain and in-plane strain. A thickness-dependent database is established by LF finite element analysis simulation, and the heating conditions are determined by matching the ratio of bending strain to in-plane strain between the required values and the laser forming values found in the database. The approach is validated by numerical simulation and experiments using several typical shapes.
[DOI: 10.1115/1.2162912]

Keywords: laser forming, varying thickness, process synthesis, bending strain

1 Introduction

Laser forming is a flexible forming process that can be used to form components into relatively complex shapes without the necessity of ancillary tooling. Significant progress has been made in analyzing the mechanism of laser forming in recent years. However, the inverse problem, which is to design process parameters (laser scanning paths and heating conditions) for a desired shape, has not been sufficiently addressed. Although the methodology of process design has been improved from simple empirical methods to physics-based methods that analyze the curvature or strain fields of the desired shape, no general process-planning scheme for general curved shapes is available due to the computational complexity of the inverse solutions to this thermal elasto-plastic problem. In order to advance the laser forming process further for realistic forming application, the process design for varying thickness plate needs to be developed.

Among the proposed methods of process planning of laser forming, one kind of approach is based on optimization theory. Yu et al. [1] introduced a novel method based on optimization theory and deferential geometry to determine the minimal strain energy required to flatten the desired shape into a flat shape. This surface development algorithm is illuminating for heating path planning, however, it does not provide an explicit method on how to determine laser paths nor on how to determine heating conditions. Liu and Yao [2] proposed a response surface methodology based optimization method for laser forming (LF) process design to make the design more robust. Another kind of approach is based on differential geometry and the curvature of the desired shape. Liu et al. [3] developed a methodology which defined the heating directions normal to the direction of the maximum principal curvature. Edwardson et al. [4] proposed an iterative process design strategy which determines the scanning paths either perpendicular to the contour plots of the resultant gradient vector constant gradient values over the surface or along the contour lines of constant height of the shape. The methodology based on differential geometry only analyzes the middle surface and therefore is only suited for very thin plates. Ueda et al. [5–7] computed the required strain field by finite element method (FEM) and decomposed the strain into in-plane and bending components. The principal in-plane or bending strain directions at discrete points determine the scanning path. Cheng and Yao [8], Liu and Yao [9] developed strategies for process design of laser forming of doubly curved thin plates by considering in-plane strain only and with both in-plane and bending strain, respectively. However, their methods were only concerned with uniform thickness plate, neglecting the effect of thickness on bending strain through the plate.

In fact, whether a desired shape can be precisely formed or not depends not only on the shape curvature, but also on its thickness. In the process analysis (in part I of this paper), it is shown that the bending deformation varies with the plate thickness because the bending rigidity, peak temperature and temperature gradient change with thickness, and the bending strain plays a more important role in the thicker locations. It is also found the bending mechanism may change with thickness between the upsetting mechanism (also named the shortening mechanism [10]) and the temperature gradient mechanism (TGM). Some of the heating conditions, such as scanning speed and beam spot size, can be adjusted to achieve more uniform bending deformation. Therefore, for the process synthesis of varying thickness plate, the determination of the scanning paths should account for the variation of bending-strain effect with changing thickness. The heating conditions should be determined from a thickness-dependent heating-condition database.

In this paper, a nonuniform thickness plate is formed into several typical shapes to investigate the characteristics of in-plane

Contributed by the Manufacturing Engineering Division of ASME for publication in the JOURNAL OF MANUFACTURING SCIENCE AND ENGINEERING. Manuscript received November 7, 2005; final manuscript received November 12, 2005. Review conducted by K. F. Ehmann.

strain and bending strain. The heating paths are determined by vector averaging the in-plane strain and bending strain. The bending strain in the thicker locations is weighted more heavily because the TGM mechanism plays a more significant role in the thicker locations. A thickness-dependent database which is established by FEM is used to determine the heating conditions. Line energy (laser power/scanning speed) can be determined first by matching the required strain ratios (bending strain/in-plane strain) and the LF-generated ones in the database. Then the proper power and scanning speed can be determined by matching the in-plane strain further. The methodology is aided by the finite element method (FEM) and validated by forming experiments.

2 Problem Description and Overall Strategy

The process design of laser forming on varying thickness plate differs from that of uniform thickness plate. Not only shape curvature, but also thickness variations, need to be accounted for in determining the scanning path. The strain or strain ratio not only is a function of power and scanning speed if the beam spot size is given, but also is a function of thickness. In varying thickness plates, even under constant heating conditions (laser power, scanning speed and beam spot size) the bending mechanism may vary along the scanning path.

An overall strategy for LF on varying thickness plates is presented which involves three steps. The first step is to determine the required strain field from the initial shape to the desired shape, and then to decompose the field into in-plane and bending strain components. The second step is to determine the scanning paths by locating the paths perpendicular to the weighted averaged strain. From Part I of this paper, it is shown that the deformation mechanism may vary with the thickness, and the bending component of strain dominates in thicker locations. Therefore, the bending strain must be weighted more in the thicker locations because under the temperature gradient mechanism (TGM), laser forming is more effective at inducing bending strains. Both the shape curvature and the thickness should be considered in setting the weighting factors. This methodology will be explained more detail in the Sec. 4. The third step is to determine the heating conditions from the thickness-dependent databases established by laser forming simulation. By matching the strain and strain ratio between the required values and those of database, the laser power and scanning speed can be determined uniquely if the beam spot size and path spacing are given. Figure 1 summarizes the overall strategy for these steps.

The experiment and simulation were carried out on varying thickness plate formed into three typical shapes. The Gaussian curvatures of the middle surfaces of the three shapes are equal to zero (parabolic shape), positive (pillow) and negative (saddle), respectively, representing the general shapes classified by curvature. The shape with zero Gaussian curvature is called a singly curved surface or a developable surface, and can be formed with only bending strain. The shapes with non-zero Gaussian curvature are called doubly curved surfaces or non-developable surfaces and generally require both in-plane and bending strains to form. In the present study, although the plate thickness is not uniform, the plate can still be considered thin since the thickness, h, is much smaller than the plate dimensions, w. Large deflection theory is considered so that stretching may exist in the middle surface.

The simplified varying thickness plate geometry was chosen because the authors want to clarify the effect of the laser forming process on varying thickness plates without inducing other complexity, and at the same time without loss of the generality. Figure 2 shows the three kinds of shapes. All three shapes can be generated by a cross section in the *Y-Z* plane sweeping along the path of cubic-spline curve in *X-Z* plane. The middle surface of the desired shapes is defined as the surface which has the same distance to both top and bottom surfaces. It can be specified by $S(x,y)=A(x)+B(y)$, where $A(x)$ and $B(y)$ are cubic-spline functions. For the case 1 shape, the thickness varies linearly from

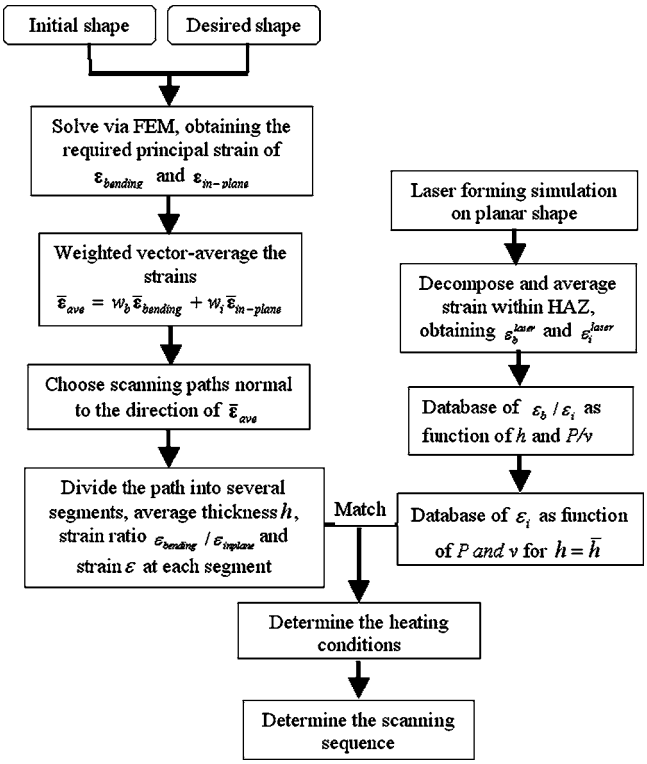

Fig. 1 Flow chart of laser forming process design for varying thickness shapes

1 to 3 mm from one edge to the other. The $B(y)$ is a straight line with two ends: (−40,−40,0) and (−40,40,0). For the pillow and saddle shape, the thickness varies from 1 to 3 mm from the edge to the center. $B(y)$ is a cubic spline defined by the three points: (−40,−40,0), (−40,0,3.5) and (−40,40,0). For the shape of case 1 and for the pillow shape, the cubic line $A(x)$ is the same, and is defined by (−40,0,0), (0, 0, 5) and (40, 0, 0). For the saddle shape, $A(x)$ is defined by (−40,0,0), (0,0,−5) and (40, 0, 0). The thickness varies only in Y direction for all these three shapes.

3 Governing Equations for Varying Thickness Plate

There are three assumptions in the current study. First, it is assumed that the straight lines, initially normal to the middle plane before bending, remain straight and normal to the middle plane during the deformation and the length of such element is not altered. This means that the vertical shear strains, ε_{xz} and ε_{yz}, are negligible, and the normal strain, ε_{zz}, is also omitted. Second, the deflection is large (>0.3 thick) and the middle plane is strained. Third, there is no abrupt variation in thickness so that the expressions for bending and twisting moments derived for plates of constant thickness apply with sufficient accuracy to the varying thickness case.

The strains can be written as the following corresponding to the displacement of midplane

$$\varepsilon_{xx} = \frac{\partial u_0}{\partial x} + \frac{1}{2}\left(\frac{\partial w_0}{\partial x}\right)^2 - z\frac{\partial^2 w_0}{\partial x^2} = \varepsilon_{xx}^s + \varepsilon_{xx}^b$$

$$\varepsilon_{yy} = \frac{\partial v_0}{\partial y} + \frac{1}{2}\left(\frac{\partial w_0}{\partial y}\right)^2 - z\frac{\partial^2 w_0}{\partial y^2} = \varepsilon_{yy}^s + \varepsilon_{yy}^b \quad (1)$$

$$\varepsilon_{xy} = \frac{1}{2}\left(\frac{\partial u_0}{\partial y} + \frac{\partial v_0}{\partial x} + \frac{\partial w_0}{\partial x}\frac{\partial w_0}{\partial y}\right) - z\frac{\partial^2 w_0}{\partial x \partial y} = \varepsilon_{xy}^s + \varepsilon_{xy}^b$$

where u_0, v_0, and w_0 are displacements of points at middle plane. ε_{xx}^s, ε_{yy}^s, ε_{xy}^s are defined as in-plane (shrinkage) strains.

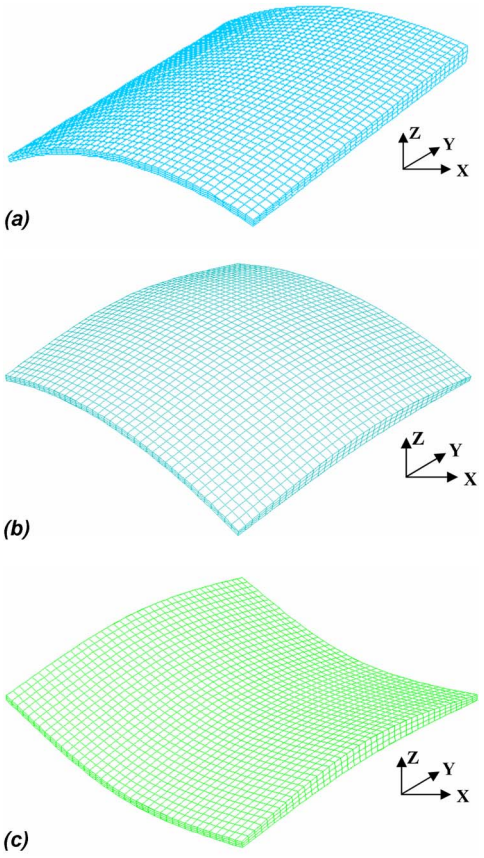

Fig. 2 Desired shapes (*a*) case 1: Gaussian curvature=0; (*b*) case 2 (pillow): Gaussian curvature>0; (*c*) case 3 (saddle): Gaussian curvature<0. All the shapes are amplified in *Z* direction (x2) for viewing clarity.

$$\varepsilon_{xx}^{b} = -z\frac{\partial^2 w_0}{\partial x^2} = z\rho_x, \quad \varepsilon_{yy}^{b} = -z\frac{\partial^2 w_0}{\partial y^2} = z\rho_y, \quad \varepsilon_{xy}^{b} = -z\frac{\partial^2 w_0}{\partial x \partial y} = z\rho_{xy}$$

are defined as bending strains, where ρ_x and ρ_y approximate the curvature along the x and y axis, respectively, and ρ_{xy} is the twisting curvature representing the warping of the x-y plane. The in-plane strain is the magnitude of the shrinkage, which is uniform through the thickness, and the bending strain is the magnitude of the shrinkage which changes through the thickness. From the definition, it is clearly shown that the bending strain is proportional to both thickness and curvature.

Noticing that for varying thickness plate, the flexural rigidity is no longer a constant but a function of thickness which is varying through the xy plane, the governing differential equations can be expressed as

$$\nabla^2\left(\frac{\nabla^2\phi}{h}\right) - (1+\nu)\left(\frac{\partial^2\phi}{\partial y^2}\frac{\partial^2}{\partial x^2}\frac{1}{h} - 2\frac{\partial^2\phi}{\partial x\partial y}\frac{\partial^2}{\partial y^2}\frac{1}{h} + \frac{\partial^2\phi}{\partial x^2}\frac{\partial^2}{\partial y^2}\frac{1}{h}\right) = E\left[\left(\frac{\partial^2 w_0}{\partial x\partial y}\right)^2 - \frac{\partial^2 w_0}{\partial x^2}\frac{\partial^2 w_0}{\partial y^2}\right] \tag{2}$$

$$\nabla^2(D\nabla^2 w_0) - (1-\nu)\left(\frac{\partial^2 w_0}{\partial x^2}\frac{\partial^2 D}{\partial y^2} - 2\frac{\partial^2 w_0}{\partial x\partial y}\frac{\partial^2 D}{\partial x\partial y} + \frac{\partial^2 w_0}{\partial y^2}\frac{\partial^2 D}{\partial x^2}\right) = p_z + \frac{\partial^2\phi}{\partial y^2}\frac{\partial^2 w_0}{\partial x^2} - 2\frac{\partial^2\phi}{\partial x\partial y}\frac{\partial^2 w_0}{\partial x\partial y} + \frac{\partial^2\phi}{\partial x^2}\frac{\partial^2 w_0}{\partial y^2} \tag{3}$$

where $h(x,y)$ is the thickness varying in xy plane, $D(x,y) = h(x,y)^3/12(1-\nu^2)$ is the flexural rigidity, ϕ the stress function, E the Young's modulus.

For uniform thickness plate, h and D are constant. Therefore, the corresponding governing equations are simplified as

$$\nabla^4\phi = Eh\left[\left(\frac{\partial^2 w_0}{\partial x\partial y}\right)^2 - \frac{\partial^2 w_0}{\partial x^2}\frac{\partial^2 w_0}{\partial y^2}\right] \tag{4}$$

$$\nabla^4 w_0 = \frac{1}{D}\left[p_z + \frac{\partial^2\phi}{\partial y^2}\frac{\partial^2 w_0}{\partial x^2} - 2\frac{\partial^2\phi}{\partial x\partial y}\frac{\partial^2 w_0}{\partial x\partial y} + \frac{\partial^2\phi}{\partial x^2}\frac{\partial^2 w_0}{\partial y^2}\right] \tag{5}$$

Compared with the governing equations for uniform thickness plates, it is seen that more nonlinear and coupled terms are added in the governing Eqs. (2) and (3) for varying thickness plate. These nonlinear and coupled terms arise from the fact that the thickness and bending rigidity varies through the plate. Some simplifications can be made to solve these nonlinear equations [11]. If the deflection w_0 is small compared to the thickness, h, the nonlinear terms are negligible and the lateral load is resisted by the bending rigidity. The bending and membrane resistances to lateral displacements are of comparable magnitudes when w_0 is of the order of h, and all terms must be retained in the equations. When w_0 is large relative to h, membrane action is predominant, and the terms containing D may be neglected.

4 Strain Field Determination

Both the FEM and the geometrical method can be used to generate the strain field required to develop a desired shape from a planar shape, but the former gives a complete strain field throughout the plate, while the latter typically gives in-plane strain for a surface only. In this case, the strain field was obtained by placing the desired shape between two rigid frictionless surfaces and then pressing it into a flat shape. This process is the opposite of developing a planar shape to the desired shape and therefore the obtained strain field has an opposite sign to that required during the forming process.

As indicated in Sec. 3, the strain field can be decomposed into two components: in-plane strain and bending strain. The in-plane strain is also called shrinkage or membrane strain in some of the literature [12]. Since the bending strain is proportional to a product of position in the thickness direction, z, and the curvature at that point, bending strain varies through the thickness. If the center of bending is located at the middle surface, the bending strain is zero at the middle surface. The in-plane strain is uniform through the thickness, therefore the strain at the middle surface is the required in-plane strain. The difference of the strain field between the top surface and the middle surface is the bending strain for the required shape.

In a general 3D space, the bending strain field (tensor) is obtained by

$$\mathrm{E}^b = \mathrm{E} - \mathrm{E}^s \tag{6}$$

where $\mathbf{E}$ is the 3×3 strain tensor at a material point on the top surface and $\mathbf{E}^s$ is the 3×3 strain tensor at a corresponding material point in the middle surface. Once the tensor of bending strain and in-plane strain is obtained, the principal values can be calculated by the eigenvalue problems

$$\mathbf{E}^s\mathbf{n}_\mathbf{i}^\mathbf{s} = \varepsilon_i^s\mathbf{n}_\mathbf{i}^s \text{ and } \mathbf{E}^b\mathbf{n}_\mathbf{i}^b = \varepsilon_i^b\mathbf{n}_\mathbf{i}^b \quad i = 1,2,3 \tag{7}$$

where ε_i are the principal strains, $\mathbf{n}_i$ the corresponding directions. It should be noted that $\mathbf{n}_i^b$ is not necessarily equal to $\mathbf{n}_i^s$.

Figure 3 compares the required strain field of singly curved shapes (case 1) with uniform and varying thickness, respectively. For the singly curved surface, only bending strain is needed to obtain the required geometry. From Figs. 3(*a*) and 3(*b*), it is clearly shown that the in-plane strains for both cases are almost zero. Figure 3(*c*) shows the bending strain in the uniform thickness shape. Since the thickness is uniform, the bending strain is uniform along the Y direction which has constant curvature, and increases from the edge to the center along the X direction where the bending curvature (although the Gaussian curvature is 0) in-

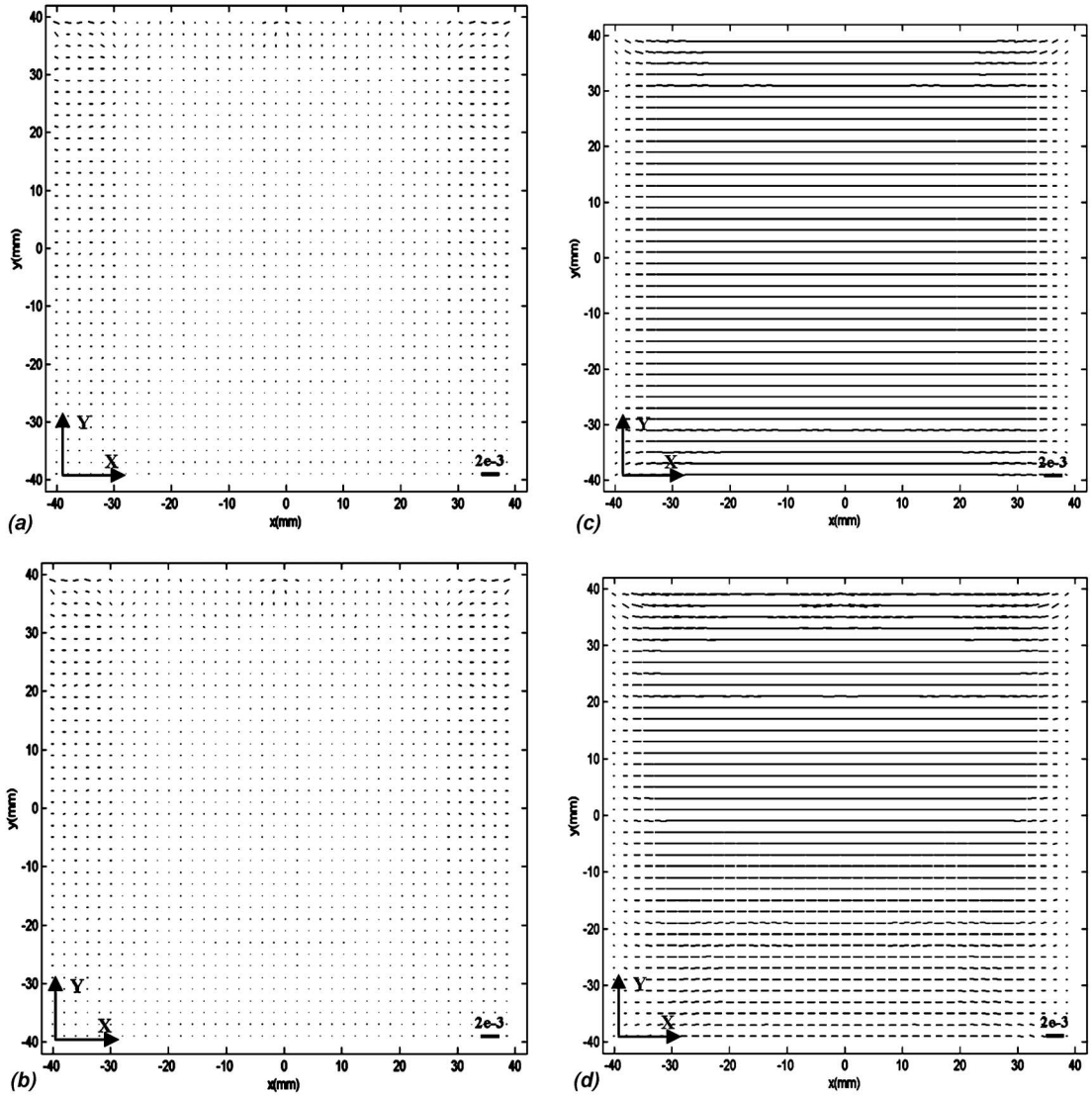

Fig. 3 Principal minimum in-plane strain for the case1 shape (*a*) with uniform thickness (*b*) with varying thickness; and principal minimum bending strain for the case 1 shape (*c*) with uniform thickness (*d*) with varying thickness plate

creases along that direction. From the distribution of bending strain in the varying thickness shape which is shown in Fig. 3(*d*), it is seen that the bending strain also increases in *Y* direction due to the increase of thickness along that direction.

Figure 4 shows the in-plane strain and bending strain for desired shapes (pillow and saddle) with varying thickness, respectively. Compared with the strain of the same geometries with uniform thickness, it is seen that the in-plane strain does not change even as the thickness varies, but the bending strain increases with the increasing thickness. To match the requirement of both in-plane and bending strain, the effect of thickness must be considered.

5 Determination of Scanning Paths

Due to the simplicity of singly curved shape, in this section we only focus on the doubly curved shapes (pillow and saddle) to investigate the scanning path determination strategy. As we know, the doubly curved shapes require both in-plane and bending strain, and laser forming generally results both in-plane and bending strains [8,9]. By examination of experimental data, it is found the highest compressive strains occur in a direction perpendicular to a scanning path. Ueda [5] proposed that the heating path should be perpendicular to the maximum principal in-plane strain where the magnitude of the in-plane strain is much larger than that of the bending strain, and perpendicular to the maximum principal bending strain direction if the magnitude is opposite. This is reasonable for very thin plates in which the bending strain is very small or for very thick plates in which the bending strain is much larger. For varying thickness plate in the present study, there are sizable bending strains and in-plane strains at the locations with larger thickness and larger curvature. It is therefore more reasonable to vector average the direction of principal in-plane strain and principal bending strain [9]. Since the effect of bending strain and in-plane strain varies with thickness and curvature, the different weight of each component should be considered during the vector averaging. The scanning paths are located perpendicular to the averaged directions.

From the process analysis in Part I, it is found that the bending strain plays a more important role in the thicker locations where the temperature gradient mechanism (TGM) tends to dominate. Ueda [5] investigated the relation between in-plane strain and bending strain and pointed out that maximum bending strain is proportional to the product of thickness and curvature, and the maximum in-plane strain is proportional to the square of curva-

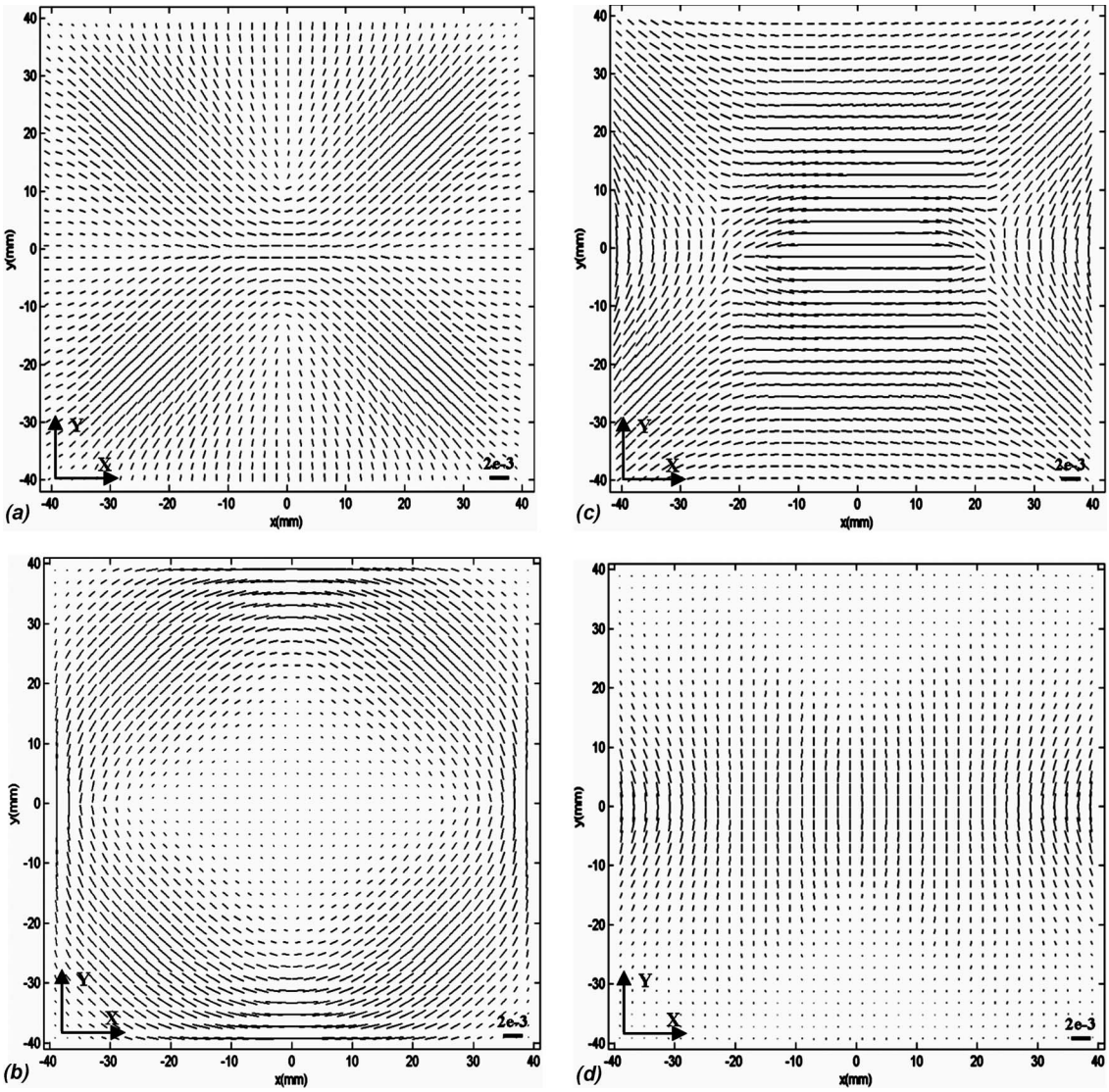

Fig. 4 Vector plot of in-plane strain of the (*a*) pillow shape with varying thickness, (*b*) saddle shape with varying thickness; and vector plot of bending strain of the (*c*) pillow shape with varying thickness, (*d*) saddle shape with varying thickness

ture. McBride et al. [13] also proposed that paraboloid curvature varies as the square root of membrane strain. Therefore, the ratio of bending strain to in-plane strain can be expressed as

$$\varepsilon_B/\varepsilon_I \propto t/\rho \tag{8}$$

where t is the thickness, and ε_B and ε_I are components of the bending and in-plane strain tensors, respectively; ρ is the surface curvature along the corresponding direction to the strain. If the principal strain value is used in the above equation, ρ is taken as Gaussian curvature which is the product of maximum and minimum principal curvature. From above relation, it is illustrated that in general the bending strain is more effective as thickness increases, and the in-plane strain is more effective as curvature increases. To utilize this relationship for later analysis, a weighted vector-averaging scheme can be adopted as

$$\bar{\boldsymbol{\varepsilon}}_{\text{ave}} = w_B\boldsymbol{\varepsilon}_B + w_I\boldsymbol{\varepsilon}_I = \left[1 + \frac{(t-\bar{t})}{\bar{t}}\frac{\bar{\rho}}{\rho}\right]\boldsymbol{\varepsilon}_B + \left[1 - \frac{(t-\bar{t})}{\bar{t}}\frac{\bar{\rho}}{\rho}\right]\boldsymbol{\varepsilon}_I \tag{9}$$

where ε_B and ε_I are principal bending strain and in-plane strain, respectively; t and $\bar{t}$ are local thickness and average thickness, respectively; ρ and $\bar{\rho}$ are the absolute value of local Gaussian curvature and average Gaussian curvature of the middle surface, respectively. For the uniform thickness ($t=\bar{t}$) shape, the weight number is equal to 1 and the above equation turns out to be the normal vector averaging method which is adopted in Liu and Yao [9].

Figures 5(*a*) and 5(*b*) show the vector averaged principal minimum strain of a pillow shape and a saddle shape, respectively. Since in TGM laser forming the plate bends towards the laser beam, the scanning path should be located on the concave side. The vector averaged principal minimum strain is used because of the compressive strain generated by laser forming. Figures 6(*a*) and 6(*b*) show the scanning paths of pillow and saddle shape, respectively. These scanning paths are only located on the bottom surface. For the saddle shape, the double curvature geometry requires that the heating paths be located on both sides of the surface, and for the heating paths on the top side, the maximum principal strain should be used with the same procedure.

In determining the spacing of adjacent scanning paths, a number of guidelines are followed. In general, the paths at the regions that have larger strains should have denser spacing than regions of smaller strains. At the same time, due to the practical restrictions

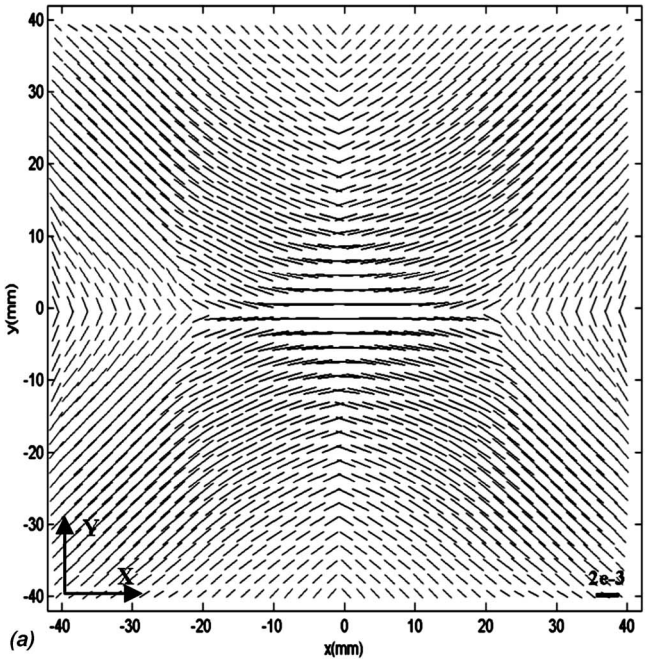

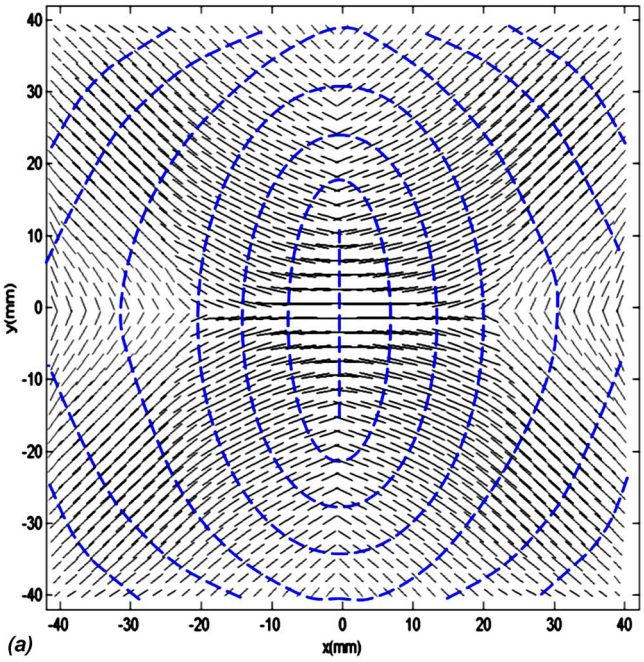

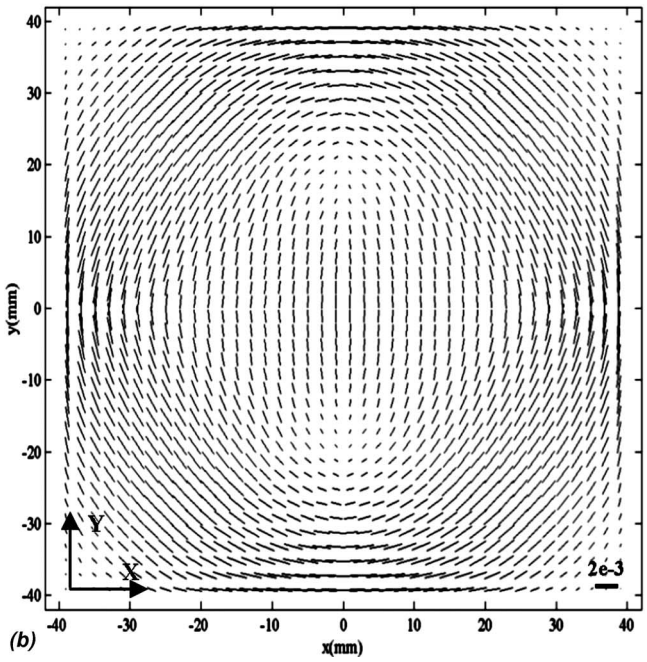

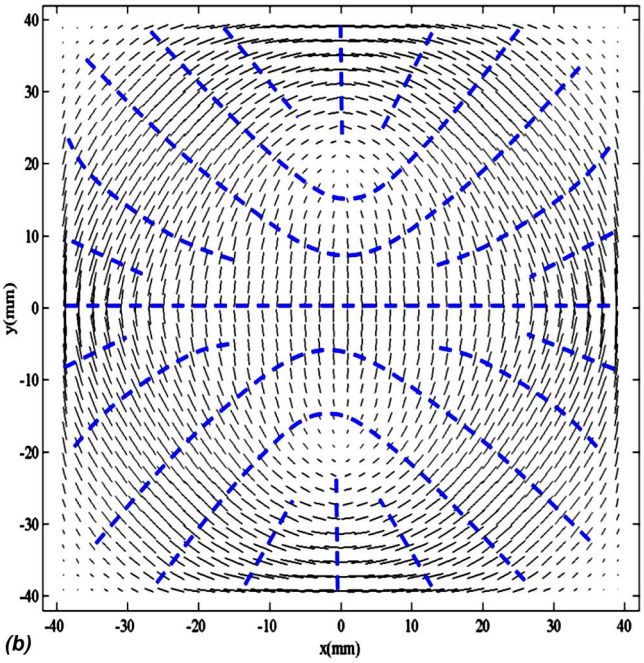

Fig. 5 Vector plot of the averaged in-plane strain and bending strain of the (*a*) pillow shape, and (*b*) saddle shape, both of which have varying thickness along the *Y* direction

Fig. 6 Determined heating paths of (*a*) pillow shape, and (*b*) saddle shape, both of which have varying thickness along the *Y* direction

such as the cooling issues, the spacing cannot be too close. Cheng and Yao [8] presented that the spacing between two adjacent paths, d_{paths}, should be equal to the average strain generated by laser forming, $\bar{\varepsilon}_{\text{laser}}$, multiplied by the beam spot size d, and divided by the required strain over the spacing, written as $d_{\text{paths}} = \bar{\varepsilon}_{\text{laser}} d / \bar{\varepsilon}_{\text{required}}$. This strategy is difficult to implement because $\bar{\varepsilon}_{\text{laser}}$ is determined by the heating conditions (including laser power, scanning speed and beam spot size) that are as yet unknown. And $\varepsilon_{\text{required}}$ is an averaged strain between the paths, and is also unknown.

If the laser generated plastic strain $\varepsilon_{\text{laser}}$ can fully match the required strain within the range of the heat affected zone (HAZ), the width of HAZ can be adopted as the initial path spacing. The spacing of the paths will vary along the paths because the paths are along directions perpendicular to the strain field which varies. If this strategy results in a path spacing that is too large to be covered by LF-generated strain, additional scanning paths should be added.

In laser forming, the strain is localized along the scanning path while the required strain field is generally continuous throughout the shape. Therefore, the average strain generated by laser forming, $\bar{\varepsilon}_{\text{laser}}$, should be obtained by integration of the plastic strain over the width of the HAZ and dividing by the width of the HAZ.

$$\bar{\varepsilon}_{\text{laser}} = \frac{1}{w^p} \int_0^{w^p} \varepsilon_y^p dy \tag{10}$$

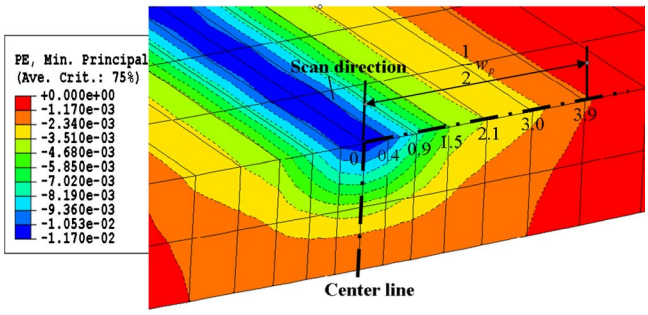

Fig. 7 Averaged plastic strain obtained from laser forming simulation through the thickness direction at a typical location (thickness=2 mm, beam size=8 mm) (the color contour shows the distribution of plastic strain in the cross section)

Figure 7 shows the distribution of $\bar{\varepsilon}_{\text{laser}}$ through the thickness. The difference of the compressive plastic strain between the top and middle surface is defined as bending strain and it is almost linearly distributed through the thickness. From the contour plot of the plastic strain distribution along Y direction, it can be seen that the width of heat affected zone, w^p, is roughly equal to the beam spot size, d, so that beam spot size can be used as the width of the plastic deformed zone.

6 Heating Conditions Determination

After determination of the scanning paths, the heating conditions need to be determined that include laser power and laser scanning speed if the beam spot size and work material are given. While it is possible to continuously vary parameters to generate a heat path plane to form the desired shape, this study adopts the strategy of constant power and piecewise constant speed for a given path for implementation simplicity. The procedure is summarized below. A path is broken down to a few segments such that within each segment, the range of strain variation (maximum minus minimum vector-averaged strain) is about the same as in other segments. Since the thickness varies through the segments, average thickness is assumed within each segment.

For each segment, laser forming conditions are chosen such that the in-plane and bending strains obtained by laser forming are equal to the required in-plane and bending strains. It should be noted that the in-plane and bending strains we refer are in fact the principal strain values that are vector averaged within the range of beam spot size. Figure 8 shows the distribution of compressive plastic strain along a centerline scanning path. It is seen that under constant laser power and scanning speed, the bending strain, which corresponds to the strain difference between top and middle surfaces, decreases first then remains nearly constant when the thickness increases. The in-plane strain, which corresponds to the plastic strain in the middle surface, decreases when the thickness increases. This is because when the thickness increases, the larger heat sink makes the peak temperature decrease, so that the generated plastic strains on both top and middle surfaces decrease. When the thickness further increases, the increasing of temperature gradient through thickness impedes the decrement of bending strain, but the in-plane strain still decreases. Therefore, the ratio of bending strain to in-plane strain increases with the thickness.

Figure 9 shows the variation of the ratio of bending strain to in-plane strain when only the scanning speed varies and when only the laser power varies, respectively. When the laser power is constant and scanning speed increases, the ratio increases with the speed. This can be explained by the fact that at lower speed, more heat will be be dissipated, so heat energy is more uniformly distributed across the thickness, and therefore in-plane shrinkage will be dominant. On the other hand, the faster the speed, the less time allowed for heat to dissipate, so the temperature gradient mechanism (TGM) will be more pronounced and bending strain will be

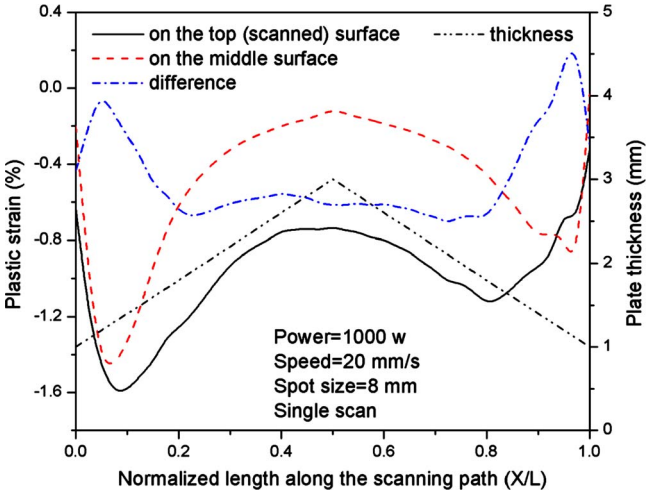

Fig. 8 Plastic strain distribution of laser forming on varying thickness plate along the scanning path (under condition of power=1000 W, scanning speed=20 mm/s, and spot size =8 mm)

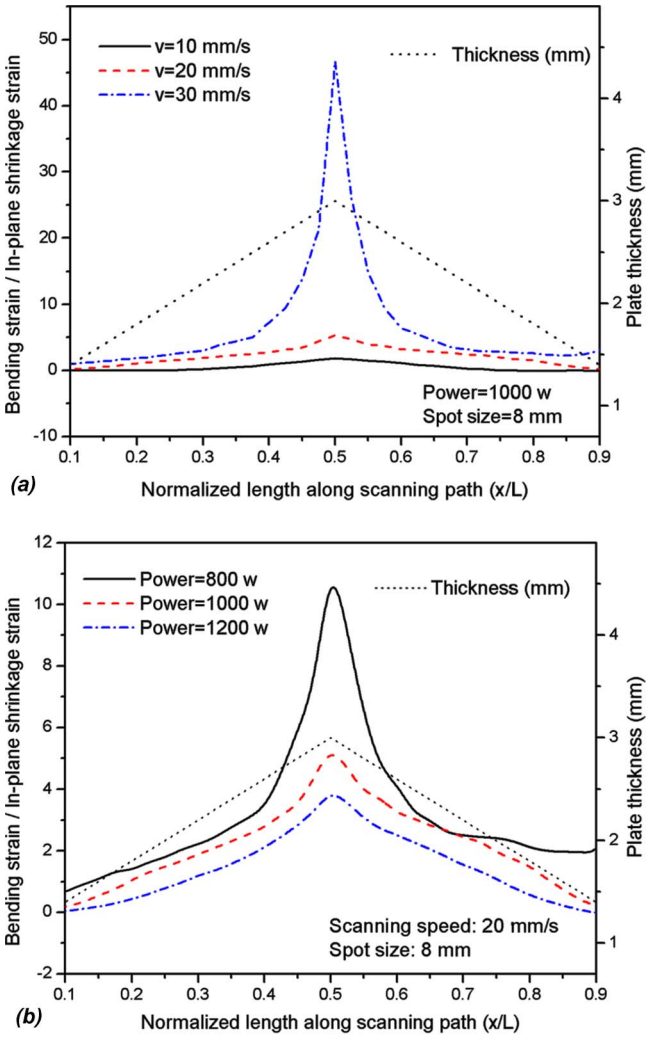

Fig. 9 Variations of the ratio of bending strain to in-plane strain with varying thicknesses (*a*) under the condition of constant power and various scanning speed; and (*b*) under the condition of constant scanning speed and various powers

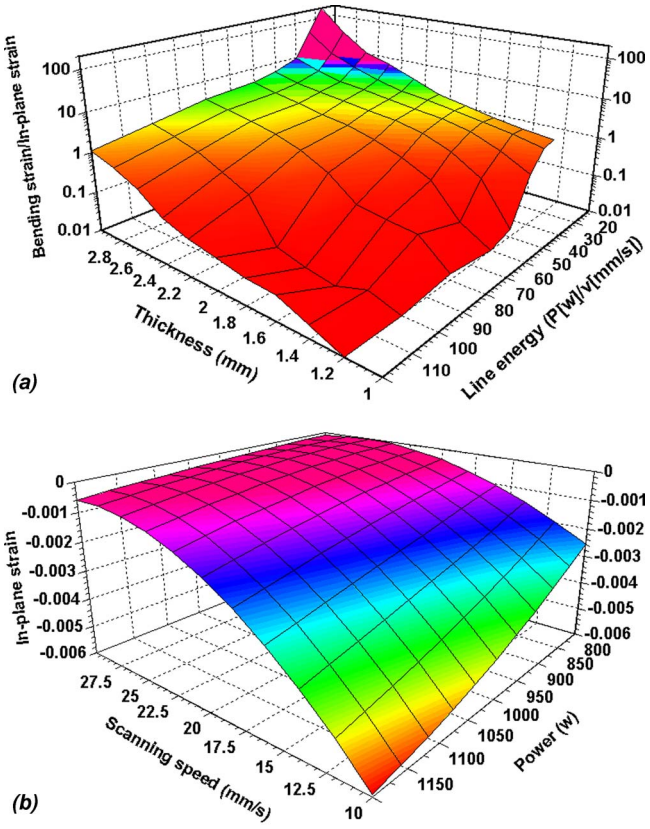

Fig. 10 Database for the determination of heating conditions (*a*) the ratio of bending strain to in-plane strain as the function of line energy (*P*/*V*) and thickness, and (*b*) the in-plane strain for a typical thickness (*h*=2 mm) as the function of power and scanning speed

more dominant. Under the higher scanning speed, the effect of the thickness on this bending/in-plane strain ratio becomes more significant. Therefore, it can be concluded that it is easier to achieve a higher ratio of bending to in-plane strain in the thicker locations under a higher scanning speed. From Fig. 9(*b*), it is seen that under constant scanning speed, when the laser power increases, the ratio decreases. This is because the increase of effective heat input with the increasing power makes the in-plane strain increase, while the bending strain does not change much. Therefore, higher scanning speed and lower laser power are helpful to obtain a higher ratio of bending strain to in-plane strain.

For varying thickness plate, if the path is divided into several segments according to the magnitude of the required strain, then the equivalent thickness, vector-averaged strain, and strain ratio for each segment can be determined. The segment having the largest strain, which has the strongest influence on the final shape, is chosen first. In determining the strain, strains between adjacent scanning paths are lumped together because all these strains are to be imparted by the paths. Compared with the *magnitude* of in-plane strain or bending strain, the *ratio* of bending strain to in-plane strain plays a more important role in determining the heating conditions. From the database of strain ratio as a function of thickness and line energy (*P*/*V*) [shown in Fig. 10(*a*)], the line energy can be determined for this segment. Then by matching the required in-plane strain with the in-plane strain in database, which is a function of power and velocity for an equivalent thickness, a group of combinations of power and velocity can be determined. The combination of power and velocity which also matches the requirement of line energy is the proper heating conditions. The determined *P* value is adopted for the entire path. For other segments in this path, since the power has been determined, the corresponding scanning velocity can be determined from the database of strain ratio as a function of thickness and line energy. It should be noted that there might be a discrepancy of the strain magnitude between the required values and the laser forming values for segments other than the first one. The reason is because the heating conditions for those segments are only determined by strain ratio and the corresponding line energy, so that the chosen conditions cannot match both the ratio of bending to in-plane strain, and the magnitude of strain simultaneously. It is believed that discrepancy can be eliminated by iterative laser forming [4] if it cannot be ignored.

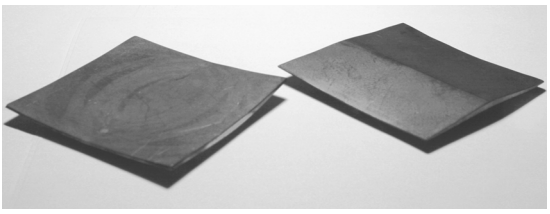

Fig. 11 Laser formed pillow and saddle shapes with varying thickness

Experiments were conducted on AISI 1010 steel coupons with dimension 80 mm by 80 mm and varying thickness (from 1 to 3.2 mm) through the *Y* direction. The scanning paths and heating conditions in the experiments were determined as described above. The laser system used is a PRC-1500 CO_2 laser, which is capable of delivering 1500 W laser power and the laser beam diameter on the top surface of the workpiece is 8 mm. Motion of the workpieces was controlled by a Unidex MMI500 mo-

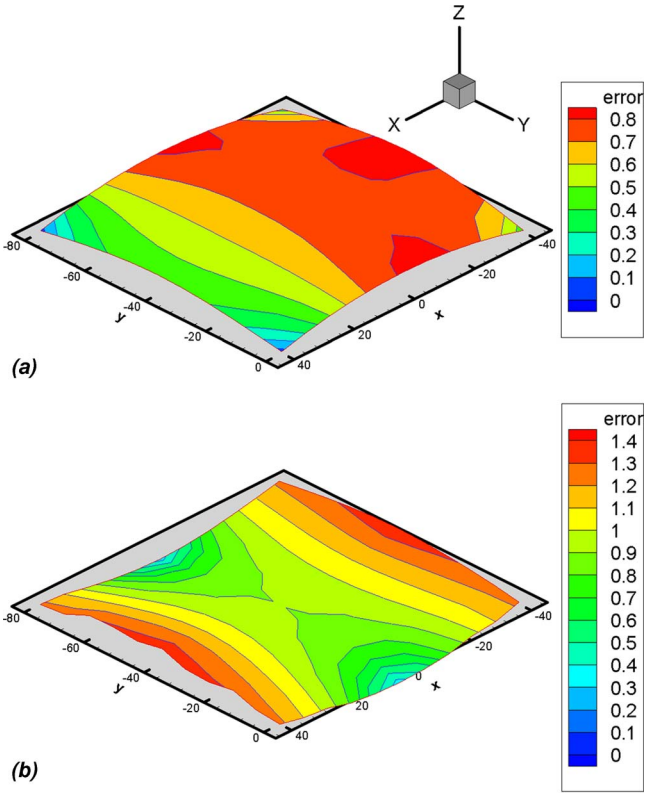

Fig. 12 Deviations of top-surface geometry between the formed shape and the desired shape for (*a*) pillow shape, and (*b*) saddle shape. The formed plates were measured by CMM and the error unit is mm.

tion control system, which allows easy specifications of variable velocities along a path with smooth transitions from segment to segment.

Figure 11 shows the formed pillow shape under these conditions. A coordinate measuring machine (CMM) is used to measure the geometry of the formed shapes. Figure 12 compares the geometry of formed shape under the prescribed processing conditions and the desired shape. In forming the saddle shape, each side of the sheet metal is scanned alternatively, i.e., scanning a path on a side, then scanning a path on the other side, and so on to achieve both the thermal symmetry and the geometry symmetry to the maximal possible extent. Only the top surface of the plate is measured and compared. A general agreement can be seen from the figures. Possible sources contributing to the discrepancy include the lumped method used to sum strains between adjacent paths; finite number of paths to approximate a continuous strain field; and constant power within each path and constant velocity within each segment.

7 Conclusions

A laser forming process design methodology for thin plates with varying thickness is presented. The strain field required to form a desired doubly curved shape is obtained through FEM, and then decomposed into in-plane and bending components. The scanning paths are located perpendicular to the directions obtained by weighted vector averaging the principal in-plane and bending strains. The weighted vector-averaging method is useful to consider the variation of bending strain with the thickness. In determining heating conditions, the relationship between the ratio of bending strain to in-plane strain to the thickness, laser power, and scanning speed was investigated. A database of the strain ratio as the function of laser power, scanning speed and the plate thickness is established. The presented methodology is validated by experiment.

Acknowledgment

The authors acknowledge the support of the NIST and of coworkers within the NIST-sponsored project "Laser Forming of Complex Structures" (Grant No. ATP-00005269).

References

[1] Yu, G., Patrikalakis, N. M., and Maekawa, T., 2000, "Optimal Development of Doubly Curved Surfaces," J. Lond. Math. Soc., **17**, pp. 545–577.
[2] Liu, C., and Yao, Y. L., 2002, "Optimal and Robust Design of Laser Forming Process," Trans. NAMRC/SME, **30**, pp. 39–46.
[3] Liu, C., Yao, Y. L., and Srinivasan, V., 2002, "Optimal Process Planning for Laser Forming of Doubly Curved Shapes," ASME J. Manuf. Sci. Eng., **126**(1), pp. 1–9.
[4] Edwardson, S. P., Moore, A. J., Abed, E., McBride, R., French, P., Hand, D. P., Dearden, G., Jones, J. D. C., and Watkins, K. G., 2004, "Iterative 3D Laser Forming of Continuous Surfaces," *Proceedings of ICALEO 2004*, Section D, pp. 36–45.
[5] Ueda, K. et al., 1994, "Development of Computer-Aided Process Planning System for Plate Bending by Line Heating (Report I)-Relation Between Final Form of Plate and Inherent Strain," Soc. Networks, **10**(1), pp. 59–67.
[6] Ueda, K. et al., 1994, "Development of Computer-Aided Process Planning System for Plate Bending by Line Heating (Report II)-Practice for Plate Bending in Shipyard Viewed from Aspect of Inherent Strain," Soc. Networks, **10**(4), pp. 239–247.
[7] Ueda, K. et al., 1994, "Development of Computer-Aided Process Planning System for Plate Bending by Line Heating (Report III)-Relation Between Heating Condition and Deformation," Soc. Networks, **10**(4), pp. 248–257.
[8] Cheng, J., and Yao, Y. L., 2004, "Process Design of Laser Forming for Three-Dimensional Thin Plates," ASME J. Manuf. Sci. Eng., **126**, pp. 217–225.
[9] Liu, C., and Yao, Y. L., 2003, "FEM Based Process Design for Laser Forming of Doubly Curved Shapes," ASME J. Manuf. Sci. Eng. (submitted).
[10] Timoshenko, S., and Woinowsky-Krieger, S., 1959, *Theory of Plates and Shells*, 2nd ed., McGraw–Hill, New York, pp. 303–308.
[11] Rivello, R. M., 1969, *Theory and Analysis of Flight Structures*, McGraw-Hill, New York, pp. 348–377.
[12] Clausen, H. B., 2000, "Plate Forming by Line Heating," Ph.D. thesis, Dept. of Naval Architecture and Offshore Engineering, Technical University of Denmark, Denmark.
[13] McBride, R., Gross, M., Moore, A. J., Hand, D. P., and Jones, J. D. C., 2004, "Calibration of Bending and Membrane Strains for Iterative Laser Forming of Non-Developable Surfaces," *Proceedings of ICALEO 2004*, Sec. E, pp. 71–80.